San Antonio Breast Cancer Symposium® — December 5–9, 2023

An integrated approach for comprehensive molecular and tumor microenvironment characterization of invasive lobular carcinoma

Abstract 1582800

Jason Mouabbi[1], Konstantin Chernyshov[2], Oleg Baranov[2], Vladimir Kushnarev[2], Polina Turova[2], Anna Butusova[2], Sofia Menshikova[2], Jessica H. Brown[2], Nikita Kotlov[2], Patrick Clayton[2], Krystle Nomie[2], Nathan Fowler[2], Debu Tripathy[1]

[1] The University of Texas MD Anderson Cancer Center, Houston, Texas, USA; [2] BostonGene Corporation, Waltham, Massachusetts, USA

THE UNIVERSITY OF TEXAS MD Anderson Cancer Center

Introduction

Although recent studies have shown that invasive lobular carcinoma (ILC) is associated with worse long-term outcomes compared to invasive breast cancer (BC) of no special type (NST), they are clinically treated in a similar manner. Therefore, classification approaches to help understand the molecular characteristics associated with the different BC subtypes are needed. Here, we describe an integrated analytical approach to comprehensively characterize ILC samples.

Methods

We collected genomic and transcriptomic data for 16,195 samples from 60 datasets forming a BC metacohort. Samples that were externally annotated as ILC or had an inactivated *CDH1* gene by mutation, deletion, or low expression (< −2.5 median absolute deviation [MAD] after median scaling) were defined as having an ILC histomolecular subtype **(Fig. 1 A, B)**. An internally developed algorithm based on clustering performed after gene expression analysis was used to classify the samples into five PAM50(BG) molecular subtypes: Basal-like, Luminal A (LumA), Luminal B (LumB), HER2-high, and HER2-low **(Fig. 2A)**. We performed molecular grade subtyping using methods described by Antysheva et al. [1]. For group comparison statistics, the Pearson's chi-square test was used. To evaluate the expression of biomarkers, transcriptomic data was median-scaled; the Mann–Whitney U test was used for statistical analysis **(Fig. 3)**. Using methods described by Bagaev et. al. [2], 29 functional gene expression signatures were selected, and unsupervised dense Louvain clustering was performed to identify tumor microenvironment (TME) subtypes. The tertiary lymphoid structures (TLS) gene signature was evaluated using methods described by Sautès-Fridman et al. [3].

Results

Histomolecular classification of the BC metacohort showed that 12% were ILC and 88% were NST **(Fig. 1)**. Classification into the PAM50(BG) subtypes showed that a greater amount of Luminal A samples were found in the ILC subtype (45%) compared to the NST subtype (24%) **(Fig. 2A)**. While HER2 (HER2-high and HER2-low) and Basal-like samples were also present in the ILC subtype, there was a larger percentage found in the NST subtype (P < 0.001, **Fig. 2A**). A lower molecular grade was more typical of the ILC samples compared to NST in Luminal (P = 1.35e-21, **Fig. 2B)** and Basal-like (P = 0.001, **Fig. 2C)** subtypes.

1 Figure 1. Histomolecular classification of the BC metacohort

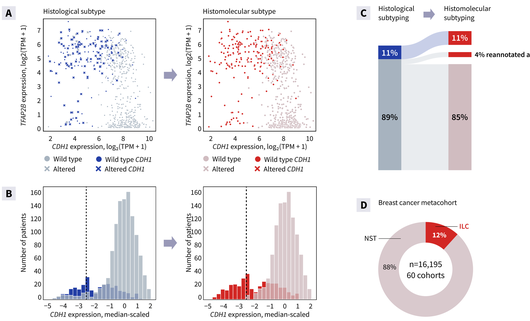

A. Improvement of the histological annotation (left) of TCGA data (n = 662) by reclassifying samples with *CDH1* alterations as an ILC histomolecular subtype (right).
B. Histomolecular classification based on gene expression, TCGA, and Metabric median-scaled data.
C. Histomolecular reclassification of cohorts with available external histological annotation.
D. Percentage of histomolecular NST and ILC samples in the BC metacohort.

2 Figure 2. Distribution of PAM50(BG) subtypes across histomolecular subtypes

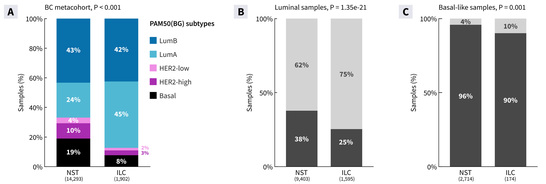

A. Presence of different PAM50(BG) molecular subtypes in NST and ILC samples.
B, C. Molecular grade subtype composition of Luminal (**B**) and Basal-like (**C**) samples in NST and ILC samples.

3 Figure 3. Expression features of ILC in different PAM50(BG) subtypes

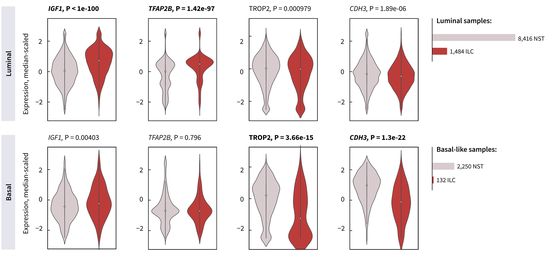

Violin plots showing the median-scaled expressions of biomarkers *IGF1*, *TFAP2B*, TROP2, and *CDH3* in Luminal (top row) and Basal-like (bottom row) samples from the BC metacohort. Histomolecular NST was compared to ILC in both Luminal (top row) and Basal-like (bottom row) samples. The Mann–Whitney test was used for statistical analysis; p-values < 1e-10 are highlighted in bold.

4 Figure 4. TROP2 expression in Basal-like ILC

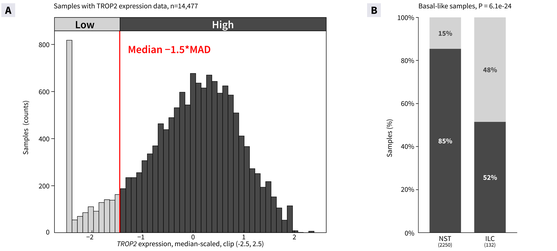

A. Median-scaled expressions of TROP2 in the BC metacohort. Samples with expressions lower than median — 1.5 x median absolute deviation (MAD) (red line on the chart) were considered low expressors.
B. Distribution of low expressors across NST and ILC in Basal-like samples.
Pearson's chi-squared test was used for statistical analysis.

5 Figure 5. Transcriptome-based TME characterization of Luminal ILC samples

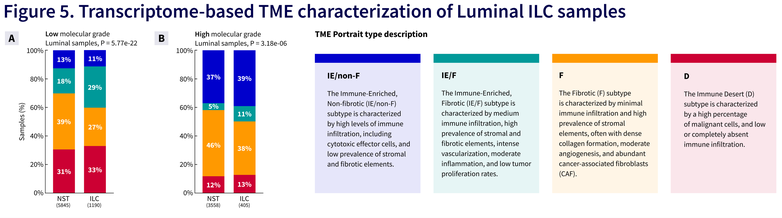

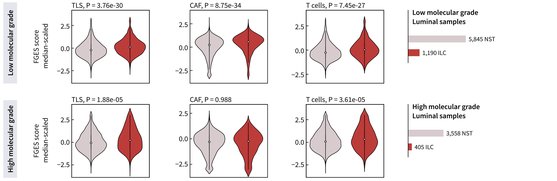

A, B. TME subtypes distribution across NST and ILC in low molecular grade Luminal samples (**A**) and high molecular grade Luminal samples (**B**). Pearson's chi-squared test was applied for statistics.
C, D. Gene signatures expression in median-scaled functional gene expression signatures (FGES). The Mann–Whitney test was used for statistical analysis.
TLS — tertiary lymphoid structures
CAF —cancer associated fibroblasts

Differences in expressions of biomarkers *IGF1*, *TFAP2B*, TROP2, and *CDH3* were revealed between ILC and NST in Luminal and Basal-like subtypes. However, while overexpression of *IGF1* (P < 1e-100) and *TFAP2B* (P = 1.42e-97) was much more common for Luminal ILC compared to Luminal NST, under-expressed TROP2 (P=3.66e-15) and *CDH3* (P = 1.3e-22) were predominant in Basal-like ILC compared to Basal-like NST **(Fig. 3)**.

TROP2 low expression outliers **(Fig. 4A)** were significantly more common in Basal-like ILC (48%) compared to Basal-like NST (15%) (P = 6.1e-24, **Fig. 4B)**, which may indicate potentially lower effectiveness of TROP2 targeted therapy in Basal-like ILC.

Transcriptome-based TME classification revealed differences in low (P = 5.77e-22, **Fig. 5A**) and high (P = 3.18e-06, **Fig. 5B**) molecular grade Luminal samples. However, a lower percentage of Immune Desert (D) TMEs and a higher percentage of Immune-Enriched/Fibrotic (IE/F) TMEs were observed in both low and high molecular grade ILC samples. TLS and T-cell signatures were overexpressed in both low (**Fig. 5C**) and high (**Fig. 5D**) molecular grade Luminal ILC samples, while the overexpression of the cancer associated fibroblasts (CAF) signature was detected only in low molecular grade Luminal ILC samples.

Conclusion

These results provide in-depth molecular and tumor microenvironment characterization of ILC. Further optimization of this analytical approach could lead to the development of more effective therapeutic strategies.

References

1. Antysheva, Zoya, et al. "Molecular-based tumor grade predictor for breast cancer, clear cell renal cell carcinoma, and lung adenocarcinoma." Cancer Research 82.12_Supplement (2022): 1227-1227.

2. Bagaev, Alexander, et al. "Conserved pan-cancer microenvironment subtypes predict response to immunotherapy." Cancer Cell 39.6 (2021): 845-865.

3. Sautès-Fridman, Catherine, et al. "Tertiary lymphoid structures in the era of cancer immunotherapy." Nature Reviews Cancer 19.6 (2019): 307-325.

Contact
Jason Mouabbi
jamouabbi@mdanderson.org

Electronic poster